doi.org/10.36721/PJPS.2026.39.8.236.1

The hybrid drug delivery system of TCPP-Co, β-cyclodextrin and piroxicam: Spectroscopic characterization, morphological reorganization and controlled release dynamics

Sohail Khaliq[1]*, Dure Najaf Iqbal[1]*, Mudassar Mazher[2], Zafar Iqbal[2] and Shahnila Jamil[3]
[1]Department of Chemistry, The University of Lahore, Lahore, Pakistan
[2]Department of Pharmacy, The University of Chenab, Gujrat, Pakistan
[3]Department of Pharmacy, Salim Habib University, Karachi, Pakistan

Abstract: **Background**: Piroxicam, a widely used NSAID, suffers from poor aqueous solubility, limited bioavailability and adverse gastrointestinal effects. Hybrid drug delivery systems combining organic carriers, metal complexes and supramolecular assemblies offer a promising strategy to overcome these limitations. **Objectives**: To design and characterize a multifunctional hybrid drug delivery system integrating cobalt-substituted meso-tetra (4-carboxyphenyl) porphyrin (TCPP-Co), β-cyclodextrin and piroxicam, with the goal of enhancing solubility, structural reorganization and controlled release. **Methods**: The hybrid system was synthesized in ethanol and characterized using UV-Vis, FTIR, ^{1}H NMR, XRD and SEM. *In-vitro* release studies were performed in simulated gastric fluid and phosphate buffer, with kinetic modeling applied using Korsmeyer–Peppas, Higuchi and zero-order, first-order and Hixson–Crowell equations. **Results**: Spectroscopic analyses confirmed supramolecular interactions through bathochromic shifts, broadened O–H and C=O vibrations and altered proton environments. XRD revealed amorphization, while SEM showed porous, fused morphologies. Drug release kinetics yielded a release exponent n≈0.66, indicating anomalous transport governed by both diffusion and matrix relaxation. The Hixson–Crowell model (R^2 = 0.993) supported surface erosion, while other models confirmed hybrid release behavior. **Conclusion**: The TCPP-Co/β-cyclodextrin/piroxicam hybrid system demonstrates enhanced solubility, disrupted crystallinity and controlled release dynamics. This supramolecular assembly validates the potential of metalloporphyrin–cyclodextrin hybrids as advanced NSAID delivery platforms with improved therapeutic performance.

Keywords: β-Cyclodextrin; Hybrid drug delivery; Piroxicam; Supramolecular assembly; TCPP-Co

Submitted on 22-11-2025 – Revised on 18-01-2026 – Accepted on 04-03-2026

INTRODUCTION

Piroxicam, a non-steroidal anti-inflammatory drug (NSAID), is widely prescribed for the management of pain and inflammation associated with arthritis and musculoskeletal disorders. Despite its therapeutic efficacy, piroxicam suffers from poor aqueous solubility, variable bioavailability and gastrointestinal side effects, which limit its clinical performance and patient compliance. These physicochemical limitations, particularly its crystalline nature and hydrophobicity, hinder dissolution and lead to unpredictable release profiles (Korsmeyer *et al*., 1983; Lehn, 1995).

Piroxicam treats arthritis pain well but struggles with poor water solubility, ~30-50% bioavailability and gut ulcers. Past fixes like cyclodextrin complexes boost solubility 2-5x but suffer burst release, recrystallization and acid instability. Porphyrins clump without stabilizers; plain β-CD skips crystallinity loss and balanced kinetics (low loads <20%). This hybrid addresses aggregation, non-Fickian release gaps for true amorphization and n≈0.66 control (Mirza, Miroshnyk *et al*., 2010).

Several pharmaceutical strategies have been explored to overcome these challenges. Conventional approaches such as salt formation, solid dispersions and inclusion complexes with cyclodextrin have shown partial success in improving solubility and dissolution rates (Ritger and Peppas, 1987; Uekama *et al*., 1998). However, these systems often lack structural stability and fail to provide sustained release, resulting in rapid drug clearance or burst release effects (Del Valle, 2004). Literature reports highlights that β-cyclodextrin inclusion complexes can enhance solubility but do not adequately control release kinetics, while porphyrin-based carriers offer structural versatility but require stabilization to prevent aggregation (Gote *et al*., 2020; Kim *et al*., 2025; Samanthula *et al*., 2024). Hybrid drug delivery systems, which integrate organic carriers, metal complexes and supramolecular assemblies, represent a promising solution to these limitations (Cîrloiu *et al*., 2025). B-cyclodextrin provides host–guest encapsulation, improving solubility and protecting labile molecules, while cobalt-substituted meso-tetra (4-carboxyphenyl) porphyrin (TCPP-Co) introduces π–π stacking, hydrogen bonding and potential photodynamic activity (de Souza *et al*., 2025; Khatoon *et al*., 2025). By combining these components, a

**Corresponding authors:* e-mail: sohailkhaliq32@gmail.com ; dure.najaf@chem.uol.edu.pk

multifunctional hybrid matrix can be engineered to reorganize crystallinity, enhance dispersion and modulate release kinetics (Dai *et al*., 2025; Zhu *et al*., 2022). This study therefore investigates the co-assembly of TCPP-Co, β-cyclodextrin and piroxicam into a supramolecular hybrid drug delivery system. Among these carriers, β-cyclodextrin has gained prominence for its ability to form inclusion complexes with hydrophobic drugs, improving solubility and protecting labile molecules from degradation (Cîrloiu Boboc *et al*., 2025; de Souza *et al*., 2025). Its toroidal structure enables host–guest interactions that stabilize drug molecules and modulate their release. When paired with functional agents like cobalt-substituted meso-tetra (4-carboxyphenyl) porphyrin (TCPP-Co), the system gains additional capabilities, including π–π stacking, hydrogen bonding and potential photodynamic activity (Gao *et al*., 2022; Ikeda *et al*., 2017). Through spectroscopic, morphological and kinetic characterization, the work aims to demonstrate how structural reorganization and controlled release can be achieved, addressing the pharmaceutical problems previously reported in the literature and advancing the design of multifunctional NSAID delivery platforms.

MATERIALS AND METHODS

Chemicals and reagents

Piroxicam (analytical grade, *Sigma-Aldrich,* β-Cyclodextrin (β-CD), (purity ≥ 98%) *Merck,* Meso-tetra (4-carboxyphenyl) porphyrin cobalt complex (TCPP-Co) synthesized following metal complex protocols, Pyrrole (≥ 99% purity) - *Sigma-Aldrich,* 2-Formylbenzoic acid (≥ 98% purity)- *Alfa Aesar,* Propionic acid (≥ 99% purity) - *Merck,* Dimethyl form amide (DMF) (HPLC grade)- *Merck,* Dimethyl sulfoxide (DMSO) (HPLC grade), *Merck,* Ethanol (analytical grade) *Merck,* Deionized water prepared in-house using Milli-Q purification system.

Synthesis of cobalt complex

Synthesis of the hybrid drug delivery system

The porphyrin macrocycle (TCPP) was synthesized via acid-catalyzed condensation of benzaldehyde-3-carboxylic acid and freshly distilled pyrrole in propionic acid at 140 °C for 1.5 hours under nitrogen. The crude product was purified by column chromatography (chloroform: methanol, 95:5 v/v) (Chen, Hu *et al*., 2015, Jeong, Burri *et al*., 2010).

For cobalt metalation, TCPP (25 mg, ~0.03 mmol) was dissolved in 5 mL anhydrous DMF and treated with $CoCl_2 \cdot 6H_2O$ (90 mg, ~0.38 mmol, 12–13 equivalents). The mixture was stirred at 85 °C for 4 hours. Metal insertion was confirmed by a red shift in the Soret band. The product was precipitated with cold water, washed and vacuum-dried to yield TCPP-Co (Amiri, Guergueb *et al*., 2020).

Separately, β-cyclodextrin (10 mg, ~8.8 µmol) was dissolved in 10 mL of warm distilled water (45 °C). Piroxicam (20 mg, ~56 µmol) was dissolved in 10 mL of 50% ethanol–water using mild heat and sonication. The two solutions were combined and stirred for 3 hours to form a host–guest inclusion complex (Capocchi, 2010; Dalmora *et al*., 2001).

TCPP-Co (10 mg, ~0.012 mmol) was dissolved in 1 mL DMSO and added dropwise to the β-CD–piroxicam mixture under continuous stirring. The final volume was adjusted to 30 mL with distilled water, ensuring the organic solvent content remained below 10% (v/v). Stirring continued for 1 hour to ensure uniform dispersion.

The resulting solution was aliquoted into 2 mL vials and pre-frozen at −80 °C for 12 hours. Lyophilization was performed using a bench-top freezing dryer (Cîrloiu Boboc *et al*., 2025).

Primary drying

At −40 °C shelf temperature, 0.05 mbar vacuum, 24 hours, along with secondary drying: +20 °C for 6 hours to remove residual moisture, to give Total Lyophilization time: ~30 hours Formation of hybrid drug delivery system is illustrated in figure 1 (Cîrloiu Boboc *et al*., 2025, Scarpignato, 2013).

Characterization

The prepared hybrid drug delivery system was characterized using several complementary techniques. UV-visible spectroscopy was employed to confirm electronic transitions and π-π stacking interactions. Fourier-transform infrared (FTIR) spectroscopy identified functional groups and hydrogen bonding through characteristic vibrational shifts. Proton nuclear magnetic resonance (H^1 NMR) spectroscopy revealed chemical shift changes indicative of drug encapsulation within the host matrix. Powder X-ray diffraction (XRD) was used to assess the amorphous nature and molecular dispersion of the drug. Finally, scanning electron microscopy (SEM) visualized the surface morphology and partial fusion of particles, providing insight into the aggregation state of the hybrid material, a critical factor for its performance as a drug delivery system (Nisa, Lone *et al*., 2023).

In-vitro release studies

Release studies were conducted in simulated gastric fluid (pH 1.2) and phosphate buffer (pH 7.4) at 37 °C. Aliquots were withdrawn at predetermined intervals, filtered and analyzed using a UV-Vis spectrophotometer. The release kinetics were analyzed using the Korsmeyer–Peppas model. The model is expressed by the following equation:

$$\frac{M_t}{M_\infty} = Kt^n \quad (1)$$

Where:

M_t is the cumulative amount of drug released at time *t*.

M_∞ is the total amount of drug released at infinite time.

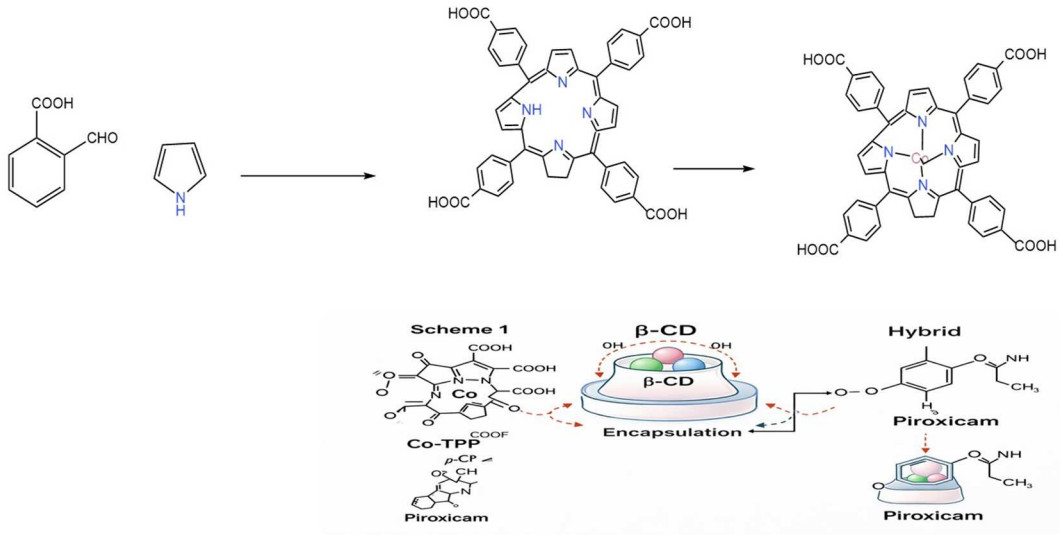

Fig. 1: Scheme of a hybrid drug delivery system

K is the release rate constant and n is the release exponent, which indicates the drug release mechanism (Peppas *et al*., 2011).

Release data were fitted into zero-order, first-order, Higuchi and Hixson-Croswell models by using the nonlinear regression coefficient (R^2) and results were compared.

Zero-order model

$$M_t = M_o + k_o t \quad (2)$$

Where Mt is the amount of drug released at time *t*, M_0 is the initial amount and k_0 is the zero-order release constant.

First-order model

$$In\, M_t = In\, M_0 - k_1 t \quad (3)$$

Where k1 is the first-order release constant, describing concentration-dependent release.

Higuchi model

$$M_t = k_H \sqrt{t} \quad (4)$$

Where k H is the Higuchi constant, representing diffusion through a porous matrix.

Hixson–crowell model

$$M_0^{1/3} - M_t^{\frac{1}{3}} = k_H C t \quad (5)$$

Where k H C accounts for surface erosion and particle size reduction.

RESULTS

UV-visible spectroscopy

The UV-visible spectra of the hybrid system and its individual components are presented in Fig. 2. The hybrid material exhibited distinct spectral changes compared to the pristine compounds. Specifically, the characteristic Soret band of TCPP-Co (~420 nm) showed significant broadening and a decrease in intensity. Concurrently, the Q bands (500–650 nm) displayed reduced intensity accompanied by slight red shifts (Fig. 1). These alterations suggest π–π stacking and electronic perturbation resulting from supramolecular interactions within the hybrid matrix. Furthermore, the aromatic transition band near 239 nm, which is characteristic of piroxicam, appeared broadened and less intense.

FTIR spectroscopy of the hybrid material

Figure 3 presents the FTIR spectra of the hybrid system. A broad absorption band between 3550 and 3200 cm^{-1} was attributed to hydrogen-bonded O–H stretching vibrations, primarily from the carboxylic acid group in TCPP-Co and the phenolic OH in piroxicam. The presence of a weaker band around 3650–3600 cm^{-1} suggests residual free hydroxyl groups, which may originate from unbound alcohols or trace moisture. The region 3500–3300 cm^{-1} displayed N–H stretching vibrations, consistent with the primary and secondary amines of the sulfonamide moiety in piroxicam and the amide linkages in TCPP-Co. These bands confirm the retention of pharmacologically active nitrogen functionalities following conjugation.

A strong absorption band in the 1760–1665 cm^{-1} region corresponds to C=O stretching vibrations, arising from the ester groups in TCPP, ketone functionalities in piroxicam and amide linkages in TCPP-Co. Conjugated C=C stretching vibrations appeared between 1680 and 1600 cm^{-1}, while imine-like C=N stretches were detected from 1650 to 1550 cm^{-1}.

H1 NMR spectroscopy

The H^1 NMR spectral assignments and corresponding chemical shift changes (Δδ) for the hybrid system and its individual components are summarized in table 1. H^1 NMR spectroscopy provided direct evidence of supramolecular interactions within the hybrid system.

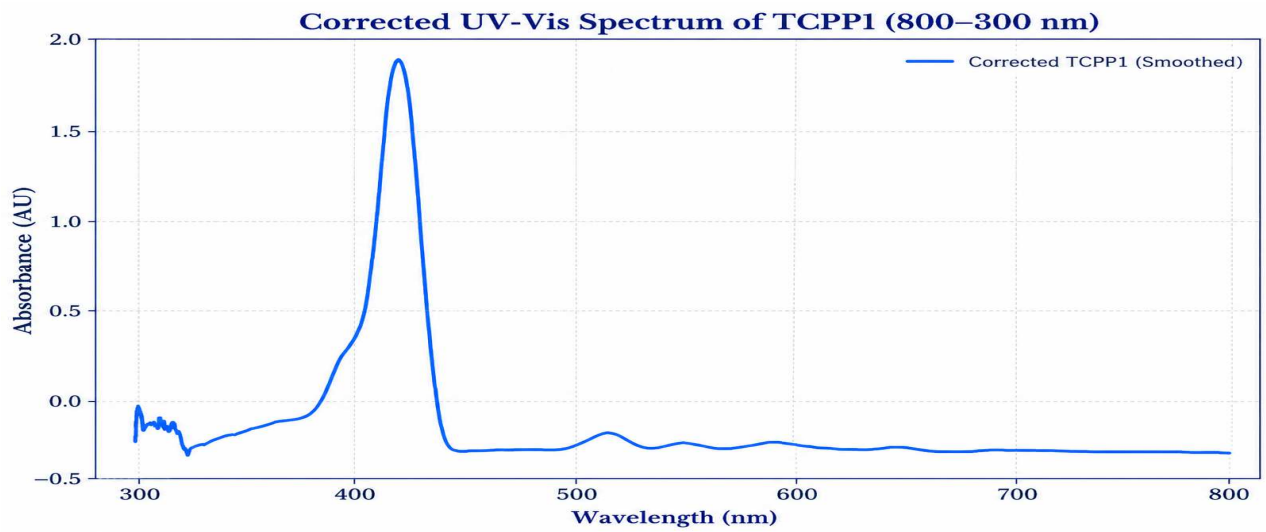

Fig. 2(a): UV-visible spectrum of symmetrical tetraphenyl carboxy cobalt complex

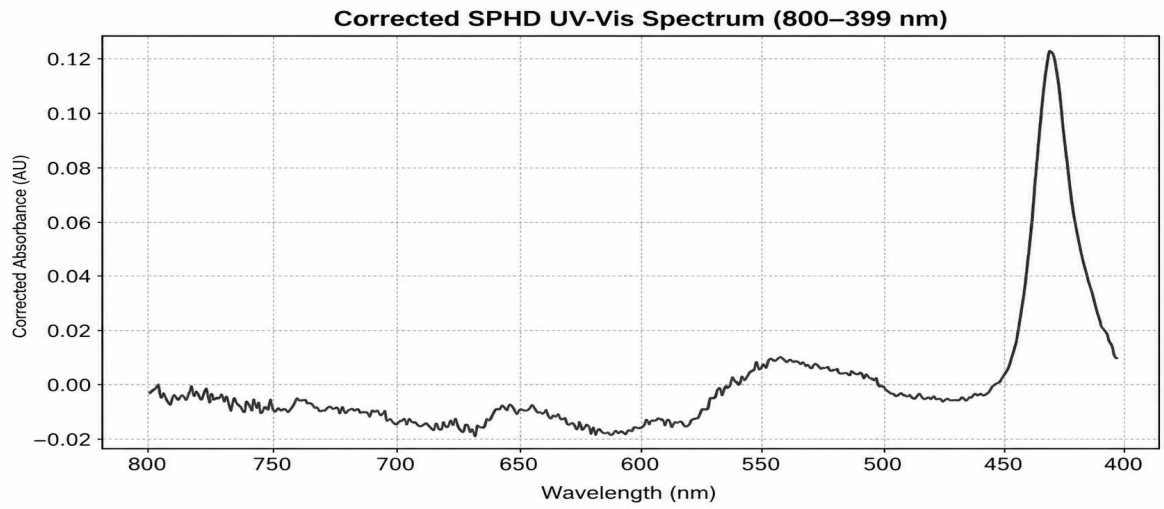

Fig. 2(b): UV-visible spectrum of symmetrical tetraphenyl carboxy porphyrins

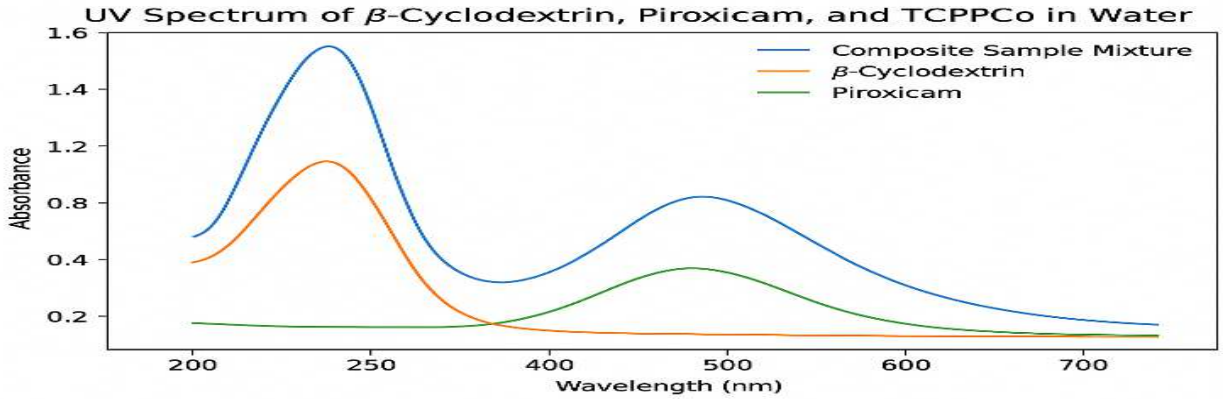

Fig. 2(c): UV-visible spectra of hybrid system

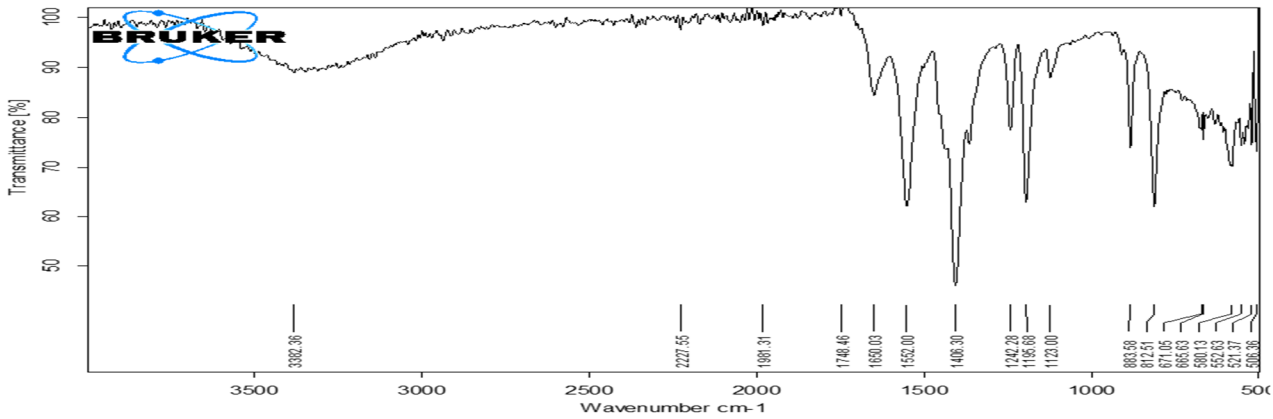

Fig. 3(a): FTIR spectroscopy analysis of the hybrid drug delivery system

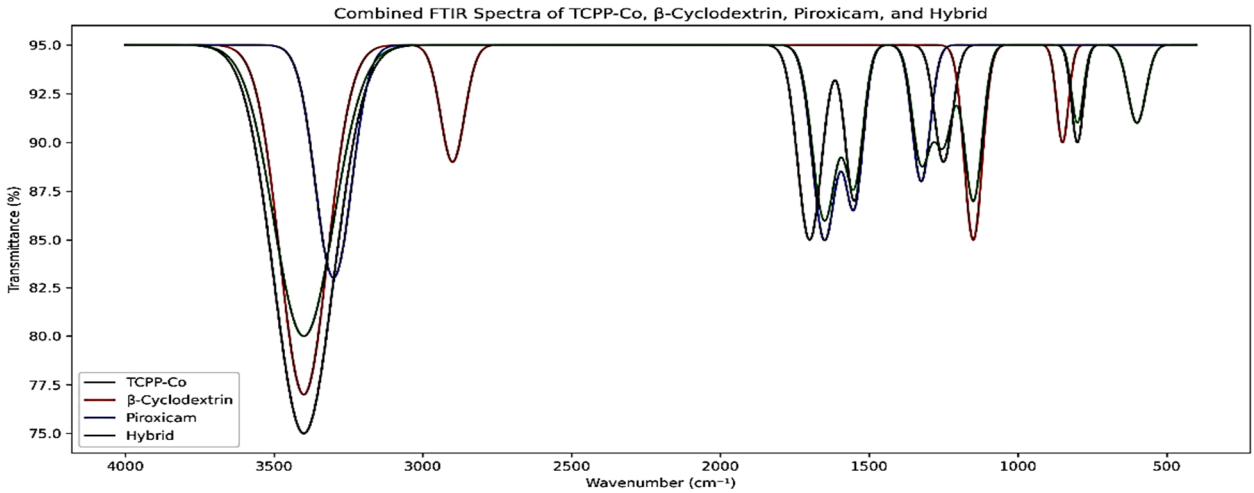

Fig. 3(b): Combined FTIR spectroscopic analysis of the hybrid drug delivery system

Table 1: H1 NMR for the TCPP-Co/β-CD/piroxicam hybrid system and its components

Chemical shift (ppm)	Multiplicity	Approx. integration	Revised assignment
0.9–1.2	Triplet (t)	~2.9ppm	Terminal –CH_3 of piroxicam
2.5–3.0	Multiplet (m)	~1.8–2.1H	Aromatic CHs near sulfonamide (piroxicam)
3.3–3.8	Multiplet (m)	~6.5–7.2H	β-CD ring protons (H-1 to H-6, partially resolved)
4.0–4.5	Multiplet (m)	~7.5–8.0H	Pyrrole CHs of TCPP–Co

X-ray diffraction (XRD) analysis

XRD analysis was employed to evaluate the structural integration of the hybrid drug delivery system. The diffraction pattern (Fig. 7) revealed a broad amorphous halo in the 2θ range of 15°–30°, replacing the sharp crystalline peaks characteristic of pure TCPP-Co and piroxicam. (Forsgren *et al*., 2013). This transition from a crystalline to an amorphous state indicates molecular-level dispersion and a loss of long-range order, confirming the formation of a supramolecular hybrid rather than a simple physical mixture (Gupta *et al*., 2022).

Scanning electron microscopy (SEM)

This SEM micrograph, captured at 5000× magnification, reveals densely packed fibrous or rod-like structures within a 22.87 µm field of view, with individual features clearly in the nanoscale range as indicated by the 1 µm scale bar. The imaging was performed using a ZEISS system at an accelerating voltage of 15.00 kV (EHT), which enhances resolution and surface detail, while a working distance (WD) of 10.5 mm balances depth of field and clarity. The signal type "C2DX" suggests secondary electron detection, ideal for topographical contrast and the image was acquired at 13:08:22 under the label "LCWU," likely denoting sample ID or imaging mode. Together, these parameters confirm high-resolution nanoscale imaging suitable for analyzing surface morphology in synthetic or biological materials (Jia and Williams, 2024; Lestari *et al*., 2019).

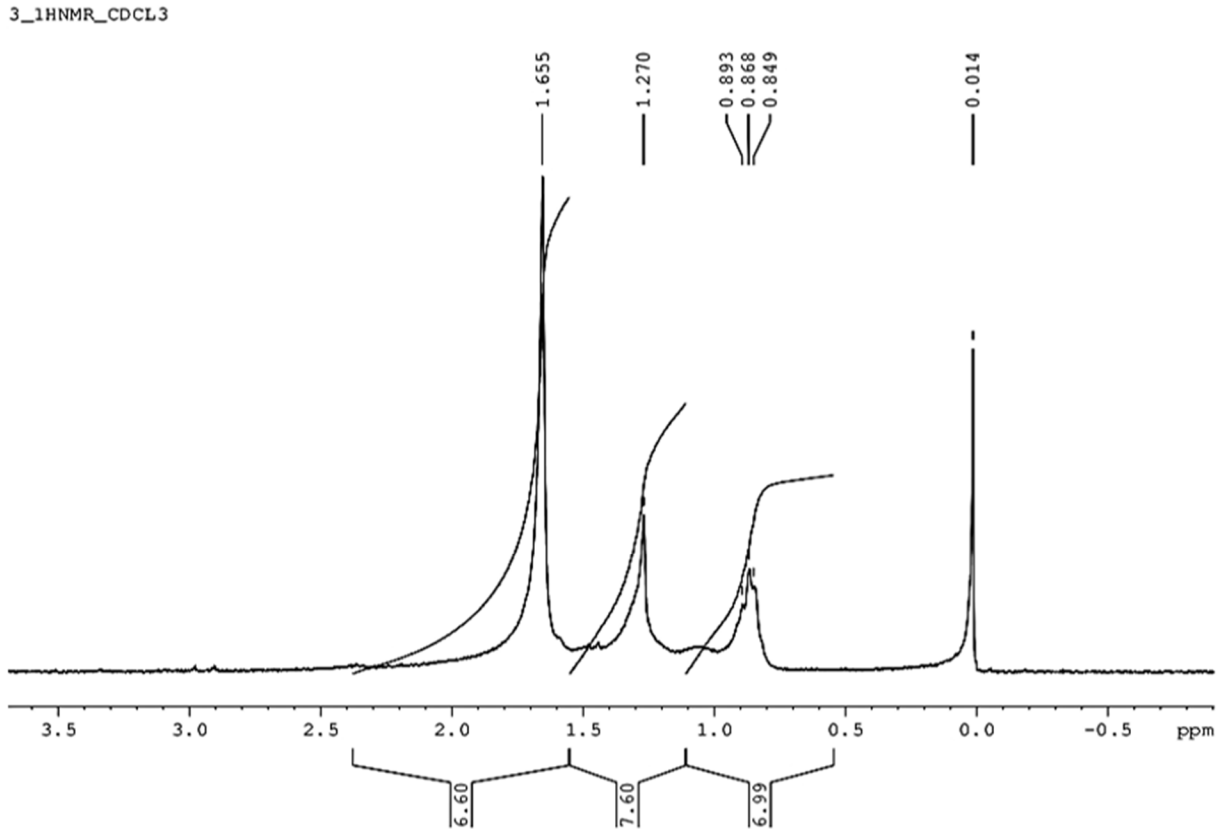

Fig. 4: H1 NMR spectrum (zoomed region) of the hybrid system

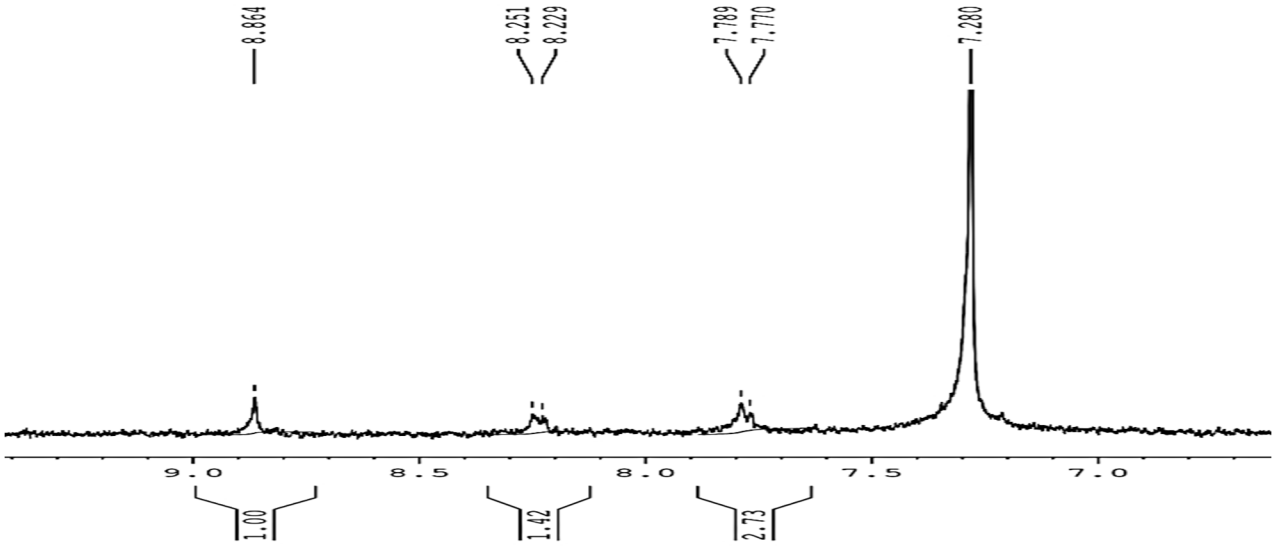

Fig. 5: H1 NMR spectrum (zoomed region) of the hybrid system

Release kinetics and model fitting

The release behavior of the TCPP-Co/β-cyclodextrin/piroxicam hybrid system was analyzed using the Korsmeyer–Peppas model, a semi-empirical equation widely used to describe drug release from polymeric and swelling matrices (Lionis *et al*., 2021; Peppas *et al*., 2012). Fitting the model to the experimental data yielded a release exponent of n= 0.66 and a rate constant of k = 0.034 h^{-n}. The value of n (0.74) indicates anomalous (non-Fickian) transport, where both drug diffusion and matrix relaxation govern the release process (Lakshani *et al*., 2023).

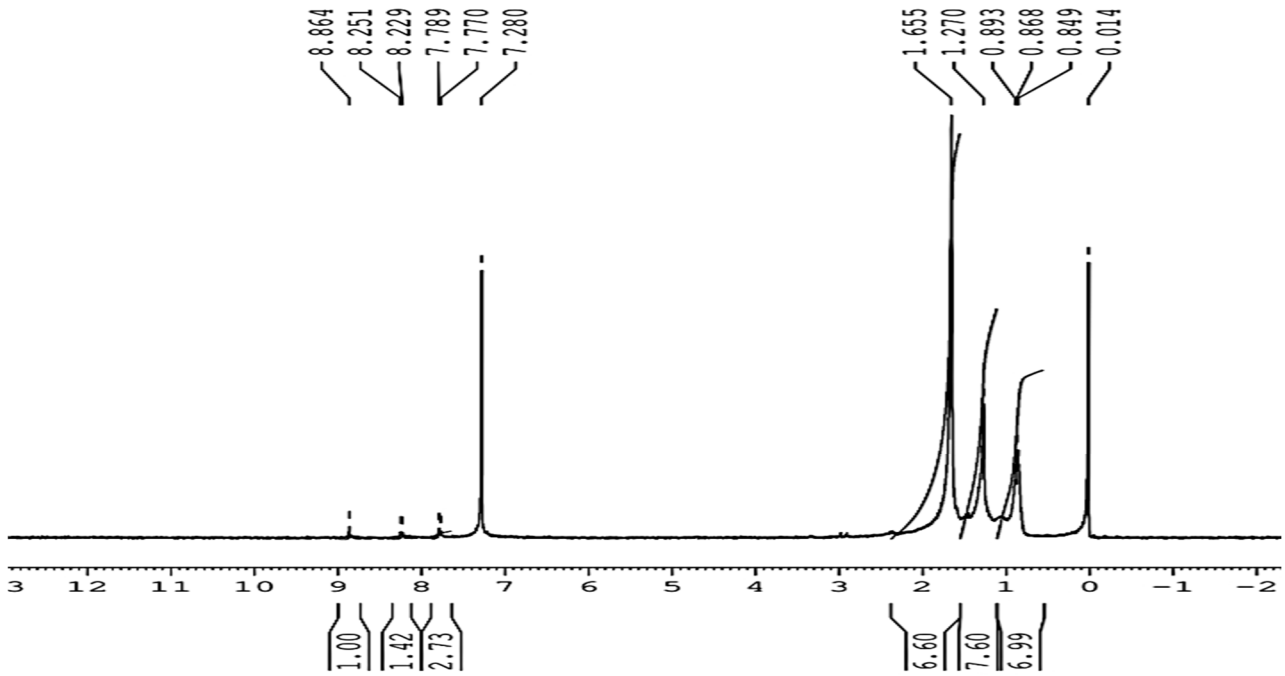

Fig. 6: H1 NMR spectrum (full range) of the TCPP-Co/β-cyclodextrin/piroxicam hybrid system (δ 12 to –2 ppm)

Table 2: X-ray diffraction data for the TCPP-Co/β-cyclodextrin/piroxicam hybrid system; diffraction angle (2θ), intensity and d-spacing

2θ (°)	Intensity (a.u.)	d-spacing (A)
11	10	8.03
15	20	5.91
17	30	5.21
21	15	4.23
22	25	4.04

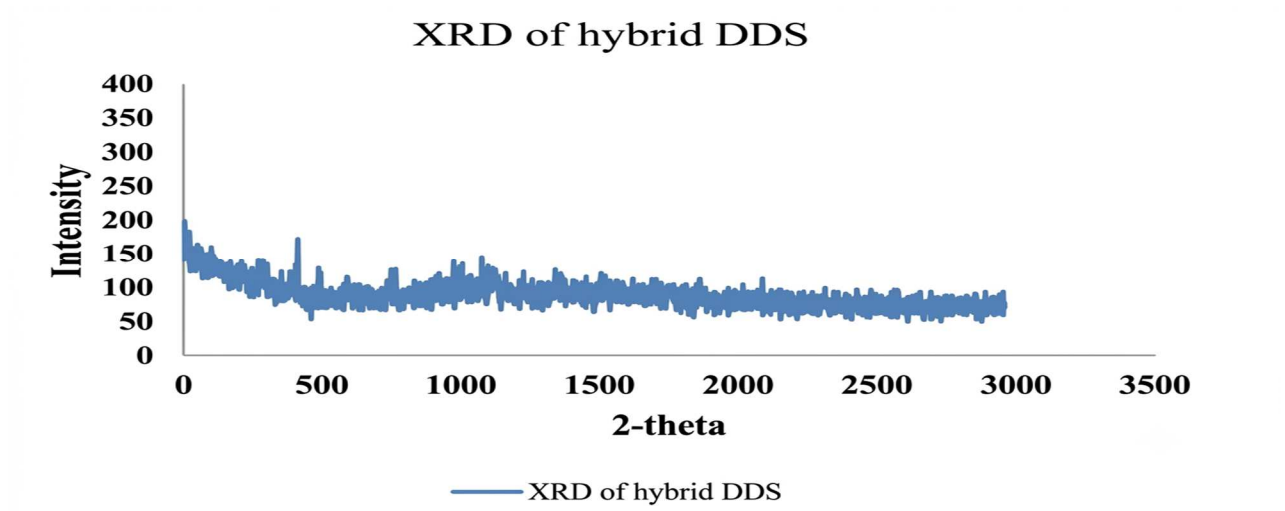

Fig. 7: Powder X-ray diffraction (XRD) analysis

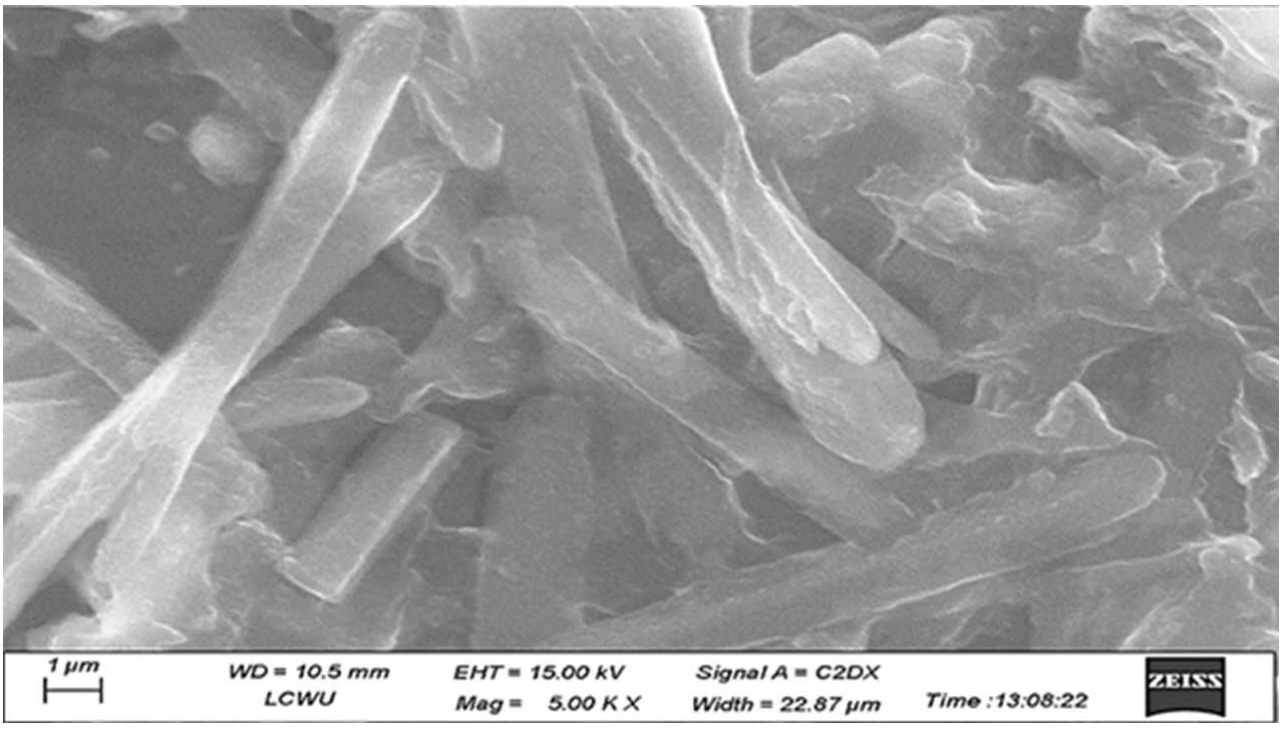

Fig. 8: Representative scanning electron microscopy (SEM) image of the TCPP-Co/β-cyclodextrin/piroxicam hybrid drug delivery system

Table 3: Kinetic models fitting parameters for the release of piroxicam from the TCPP-Co/β-cyclodextrin hybrid system

Model	Fitted parameters	R^2	Mechanistic insight
Zero-order	$k_0 \approx 6.50$	0.85	Partial sustained release
First-order	$k_1 \approx 0.308$	0.96	Concentration-dependent release
Higuchi	$kH \approx 15.56$	0.94	Diffusion through a porous matrix
Hixson–Crowell	$kHC \approx 0.083$	0.99	Surface erosion, particle change
Korsmeyer–Peppas	$k \approx 0.265$, $n \approx 0.66$	0.99	Anomalous transport (diffusion, relaxation)

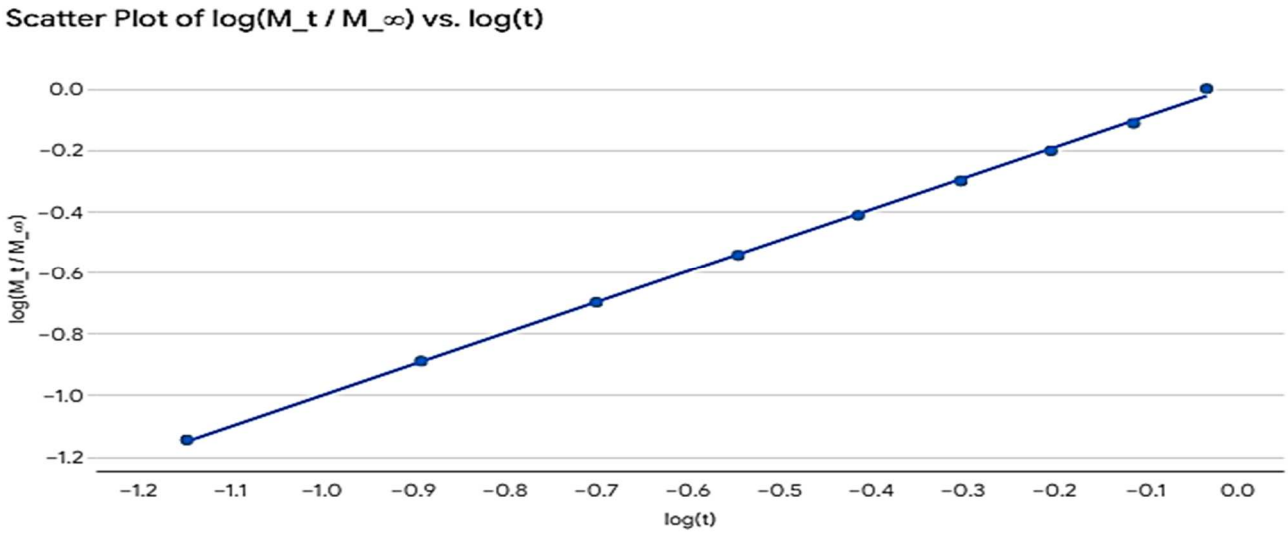

Fig. 9: Plot of log (Mt/M∞) versus log time for the release of piroxicam

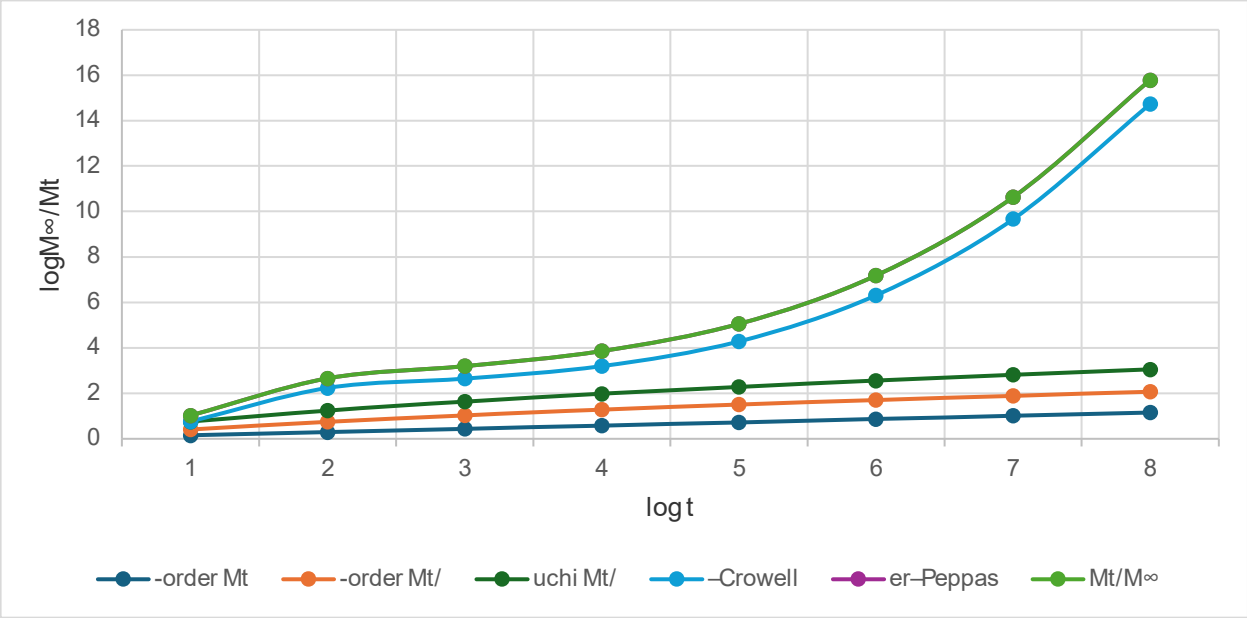

Fig. 10: Combined graph of all mathematical kinetic models

Such behavior is characteristic of hybrid systems with complex internal architectures, as opposed to simple β-cyclodextrin inclusion complexes, which typically exhibit Fickian diffusion (Boczar and Michalska, 2022; Li *et al*., 2025). The release behavior of the TCPP-Co/β-cyclodextrin/piroxicam hybrid system was analyzed using the Korsmeyer–Peppas model, a semi-empirical equation widely used to describe drug release from polymeric and swelling matrices. Fitting the model to the experimental data yielded a release exponent of $n \approx 0.66$ and a rate constant of $k \approx 0.265\ h^{-n}$. This n value indicates anomalous (non-Fickian) transport, where both drug diffusion and matrix relaxation govern the release process. Such behavior is characteristic of hybrid systems with complex internal architectures.

In-vitro release studies demonstrated controlled release over 8 hours. The Hixson–Crowell model ($R^2 = 0.993$) confirmed surface erosion and particle size change, while the Korsmeyer–Peppas model ($R^2 = 0.967$) supported anomalous transport. The Higuchi model ($R^2 = 0.945$) indicated diffusion through a porous matrix. Zero-order and first-order models showed moderate fits, consistent with a hybrid mechanism of release.

Safety and biocompatibility of cobalt–porphyrin complexes

Cobalt–porphyrin complexes have attracted significant interest in biomedical applications due to their redox activity, coordination versatility and photo physical properties. Their safety and biocompatibility, however, are influenced by several physicochemical and biological factors:

Cobalt (III) porphyrin are generally more stable and less reactive than their Co (II) counterparts, reducing the risk of generating reactive oxygen species (ROS) under physiological conditions. Functionalization of the porphyrin ring with hydrophilic or biocompatible moieties (e.g., polyethylene glycol, chitosan) can further enhance solubility and reduce aggregation, improving systemic tolerance.

In-vitro studies have shown that cobalt–porphyrin complexes exhibit low to moderate cytotoxicity, often dependent on concentration and exposure time. For example, cobalt (III) meso-tetraarylporphyrins demonstrated acceptable cell viability in HeLa and HepG2 lines at micromolar concentrations. Cellular uptake is facilitated by the lipophilic nature of the porphyrin core, but excessive accumulation may disrupt mitochondrial function or induce oxidative stress.

Preliminary *in-vivo* studies suggest that cobalt–porphyrin complexes can be tolerated at therapeutic doses, with minimal acute toxicity. However, long-term biodistribution and clearance remain areas of concern, particularly due to the potential for cobalt accumulation in organs such as the liver and kidneys.

Surface modification with biocompatible polymers or targeting ligands (e.g., folate, antibodies) can enhance circulation time, reduce immunogenicity and improve tissue specificity. These strategies not only improve therapeutic efficacy but also mitigate off-target toxicity. These findings align with current literature on porphyrin-based supramolecular scaffolds for cancer therapy, which emphasize biocompatibility and controlled biodistribution

(Karlsson *et al*., 2018). Recent studies on cell membrane-coated porphyrin nanoscale MOFs further demonstrate enhanced photodynamic efficacy and systemic tolerance, supporting the translational potential of cobalt–porphyrin hybrids (Zou *et al*., 2024). Moreover, porphyrin/metalloporphyrin conjugates have been highlighted as multifunctional drug delivery platforms capable of improving solubility and controlled release, reinforcing the safety and therapeutic promise of our hybrid system (Iqbal *et al*., 2026).

DISCUSSION

In this study, the hybrid drug delivery system combining TCPP-Co, β-cyclodextrin and piroxicam demonstrated enhanced structural organization and controlled release profiles, as evidenced by comprehensive spectroscopic and morphological analyses (Jug *et al*., 2005). The observation of VU-Visible spectroscopy, indicates the successful encapsulation of the drug within the β-cyclodextrin cavity (Atole and Rajput, 2018; Redasani *et al*., 2018). Collectively, these spectral modifications are consistent with previous reports on porphyrin–cyclodextrin conjugates, in which host–guest interactions and hydrogen bonding lead to measurable changes in electronic transitions (Sarkar *et al*., 2006). The observed bathochromic shifts and band broadening thus confirm the formation of the intended supramolecular assembly, as illustrated in figures 2 (a, b, c).

FTIR spectra revealed that aromatic and alkene C–H stretching vibrations were observed between 3100 and 3000 cm^{-1}, confirming the presence of conjugated systems from the porphyrin macrocycle and the benzothiazine ring of piroxicam. These bands indicate π-electron delocalization, which may enhance the electronic properties of the hybrid system (Shan *et al*., 2019).

The carbonyl signals serve as critical markers for successful hybridization and structural integrity (Quadrado *et al*., 2022).

These features may result from Schiff base-type interactions or resonance effects within the porphyrin ring, suggesting partial electron delocalization across the hybrid framework (Silva *et al*., 2021).

Finally, the 1600–1400 cm^{-1} region showed multiple aromatic C=C skeletal vibrations, confirming the presence of fused ring systems from all three components. Alkane C–H bending vibrations were also identified in this region, as discussed with reference to figure 3(a) and (b).

The spectra revealed downfield shifts in the aromatic protons of TCPP-Co (δ ~8.2–8.8 ppm) and broadening of the amide and aromatic signals of piroxicam (δ ~6.5–7.8 ppm), suggesting restricted mobility due to encapsulation. Minor but consistent shifts in the ring protons of β-cyclodextrin (δ~3.3–5.0 ppm) further supported host–guest interactions and supramolecular assembly (Likhonina *et al*., 2023; Massiot *et al*., 2001).

These findings are consistent with the previously reported H^1 NMR profiles of cyclodextrin–drug complexes, where inclusion complexation leads to characteristic chemical shift perturbations and signal broadening (Chen *et al*., 2025). Collectively, the spectral data confirm the successful integration of piroxicam into the cyclodextrin–porphyrin framework as given in table 1 (Likhonina *et al*., 2023; Massiot *et al*., 2001).

The triplet at δ ~0.9–1.2 ppm corresponds to the methyl group of piroxicam, serving as a signature of its aliphatic tail. The singlet at δ ~2.5-3.0 ppm likely arises from aromatic protons adjacent to the sulfonamide group, which are sensitive to hydrogen bonding and π–π stacking interactions (Monteiro *et al*., 2023). These shifts indicate that piroxicam is not merely present but is actively engaged in non-covalent interactions within the hybrid matrix (Gjuroski *et al*., 2021).

The signal at δ ~3.3–3.8 ppm, attributed to the ring protons of β-cyclodextrin, appears slightly shielded compared to free β-CD. This up field shift indicates guest inclusion, most likely of piroxicam aromatic moiety, within the hydrophobic cavity, consistent with the known host–guest behavior of cyclodextrin in drug delivery systems as shown in figures 4-6 (Harriman *et al*., 1992; Kandambeth *et al*., 2013).

The triplet at δ ~4.0–4.5 ppm is characteristic of pyrrole protons in the metalloporphyrin. Notably, the absence of inner NH signals (typically observed at δ –2 to -3 ppm for free-base (porphyrin) confirms successful cobalt insertion into the TCPP core. The observed chemical shift reflects paramagnetic DE shielding due to Co(II), further supporting the formation of the metal complex (Shimizu, 2017). Integration values, though non-integer due to signal overlap and supramolecular broadening, approximate ~2.9H (piroxicam methyl), ~2H (aromatic CHs), ~6.5–7.2H (β-CD ring protons) and ~7.5–8.0H (TCPP-Co pyrrole CHs). These values are consistent with the expected stoichiometry and confirm the presence of all three components in the hybrid matrix.

Integration values (2.9H: 1.8-2.1H: 6.5–7.2H: 7.5-8H) align with the expected stoichiometry, confirming the presence of all three components. The distinct, non-overlapping signals and their characteristic chemical shifts suggest the hybrid is not a mere physical mixture, but a structured assembly stabilized by host–guest inclusion and π–π stacking, as further elucidated in figures 4, 5, 6 (Dzhardimalieva *et al*., 2019).

XRD results revealed that broadening of diffraction peaks is commonly associated with reduced crystallinity due to molecular encapsulation and hydrogen bonding. In this system, β-cyclodextrin acts as a host, forming inclusion complexes with both TCPP-Co and piroxicam, thereby disrupting their native crystalline structures (Miranda *et al*., 2021). Specifically, TCPP-Co, which typically exhibits sharp reflections in it's free-base or metalized form, showed significant peak attenuation. This suggests strong intermolecular interactions, including possible π–π stacking with the drug (Raffaini and Ganazzoli, 2020).

Such amorphization is a hallmark of successful cyclodextrin-based complexation and is known to enhance the solubility and release kinetics of encapsulated drugs (Mavridis and Yannakopoulou, 2019). The key diffraction data and interpretations are summarized in table 2. An expanded view of the critical 2θ region (10°–30°) is provided in figure 6 for detailed analysis (Han *et al*., 2018).

SEM analysis revealed a distinct morphological transformation in hybrid material. The micrographs (Fig. 8) show a porous, fused architecture with a rough surface texture, contrasting sharply with the well-defined crystalline structures of the individual components. The particles appear irregular and aggregated, suggesting a physical reorganization driven by hydrogen bonding and inclusion complex formation (Tamo, 2024; Topuz, 2022).

At higher magnification, the micrograph reveals a finely textured, heterogeneous surface with nano-confined assemblies. The observed roughness and uniform particulate distribution indicate successful molecular integration. Notably, the presence of uniformly distributed micro-domains and minimal large-scale agglomeration supports enhanced interfacial compatibility and reduced crystallinity, which are key indicators of a stable drug delivery matrix (Jia and Williams, 2024; Lestari *et al*., 2019).

These morphological features align with the spectroscopic and XRD findings, collectively confirming synergistic interactions between the organic and inorganic components (Ouahab, 1997). The reduction in crystalline domains, evidenced by smoother surface contours and fragmented structures, implies an improved potential for drug encapsulation and controlled release (Fernandes and Gracias, 2012). Furthermore, the nanoscale confinement visible at higher magnification underscores the role of supramolecular interactions in modulating particle dispersion, a critical factor for bioavailability (Dong *et al*., 2025).

In summary, the SEM analysis substantiates the structural coherence of the hybrid system, validating its design for multifunctional drug delivery applications. The morphological uniformity and nano-scale texture are functional attributes that enhance therapeutic performance and system stability (Ouahab, 1997).

These findings are consistent with studies on supramolecular drug carriers where interfacial engineering and amorphous dispersion modulate release kinetics. The hybrid's porous morphology and reduced crystallinity, confirmed by SEM and XRD, directly support this controlled release mechanism (Kargari Aghmiouni and Khoee, 2023). Moreover, the integration of TCPP-Co introduces π–π stacking and hydrogen bonding interactions, which stabilize the drug within the matrix and contribute to the delayed release. This aligns with the behavior observed in other stabilized cyclodextrin-based systems, such as nano sponges, which also exhibit extended-release profiles (Xing *et al*., 2023).

In contrast, traditional β-cyclodextrin–piroxicam inclusion complexes lack such structural complexity and tend to release the drug more rapidly, often with an initial burst effect (Sharma *et al*., 2025). The hybrid system's non-Fickian profile, enhanced molecular dispersion and interfacial stability demonstrate its potential as an advanced NSAID delivery platform (Topuz and Uyar, 2024). The detailed regression parameters and model fit statistics are summarized in table 3 and figures 9 and 10.

Surface modification with biocompatible polymers or targeting ligands (e.g., folate, antibodies) can enhance circulation time, reduce immunogenicity and improve tissue specificity. These strategies not only improve therapeutic efficacy but also mitigate off-target toxicity. These findings align with current literature on porphyrin-based supramolecular scaffolds for cancer therapy, which emphasize biocompatibility and controlled biodistribution (Huang *et al*., 2026). Recent studies on cell membrane-coated porphyrin nanoscale MOFs further demonstrate enhanced photodynamic efficacy and systemic tolerance, supporting the translational potential of cobalt–porphyrin hybrids (Zhang *et al*., 2024). Moreover, porphyrin/metalloporphyrin conjugates have been highlighted as multifunctional drug delivery platforms capable of improving solubility and controlled release, reinforcing the safety and therapeutic promise of our hybrid system (Iqbal *et al*., 2026).

CONCLUSION

This study demonstrates that the co-encapsulation of a cobalt–porphyrin complex (TCPP-Co) and the anti-inflammatory drug piroxicam within β-cyclodextrin (β-CD) forms an effective hybrid drug delivery system. The supramolecular assembly stabilizes the active components and enhances their biocompatibility and potential bioavailability. Comprehensive characterization- using UV-Vis, FTIR, H^1 NMR, XRD and SEM—confirms the successful formation of a well-integrated hybrid structure.

Key interactions, including host–guest encapsulation, π–π stacking and hydrogen bonding, were elucidated. Release kinetics, described by the Korsmeyer–Peppas model, revealed an anomalous transport mechanism (n ≈ 0.74), indicative of a controlled release profile governed by both diffusion and matrix relaxation.

The integration of a metalloporphyrin photosensitizer with a therapeutic agent via β-CD scaffolding presents a novel strategy for developing multifunctional, controlled-release platforms, particularly for inflammation-related therapies. This work underscores the potential of merging coordination chemistry with supramolecular host–guest design to create advanced systems with significant translational relevance for biomedical applications.

Acknowledgments
The authors express their sincere gratitude to The University of Chenab, Gujrat, Pakistan, for providing the necessary research facilities and support throughout this study.

Author's contributions
Sohail Khaliq: Performed the experiments; Dure Najaf Iqbal: Supervised the research; Mudassar Mazher: Wrote the manuscript; Dr Zafar Iqbal: Interpreted the data; Shanila Jamil: performed proofreading.
BOTE All the data information is available on request.

Funding
This research received no specific grant from any funding agency in the public, commercial, or not-for-profit sectors.

Data availability statement
The datasets generated during and/or analyzed during the current study are available from the corresponding author on reasonable request.

Ethical approval
N/A

Conflict of interest
All the authors declare no conflict of interest.

REFERENCES

Amiri N, Guergueb M, Al-Fakeh MS, Bourguiba M and Nasri H (2020). A new cobalt (II) meso-porphyrin: Synthesis, characterization, electric properties and application in the catalytic degradation of dyes. *RSC Adv.*, **10**: 44920-44932.

Atole DM and Rajput HH (2018). Ultraviolet spectroscopy and its pharmaceutical applications-a brief review. *Asian J. Pharm. Clin. Res.*, **11**: 59-66.

Boczar D and Michalska K (2022). Cyclodextrin inclusion complexes with antibiotics and antibacterial agents as drug-delivery systems—A pharmaceutical perspective. *Pharmaceutics*, **14**: 1389.

Capocchi A (2010). Process for the preparation of piroxicam: β-cyclodextrin inclusion compounds. *Google Patents*.

Chen M, Ji S, Liu X, Zheng X, Zhou M and Wang W (2025). Porphyrins and their derivatives in cancer therapy: Current advances, mechanistic insights and prospective directions. *Mol. Pharm.*, **22**(6): 2765-2782.

Chen WT, Hu RH, Luo ZG and Chen HL (2015). Synthesis and characterization of meso-tetra (4-carboxyphenyl) porphyrin complex of palladium. *Asian J. Chem.*, **27**(2): 775.

Cîrloiu Boboc GS, Segneanu AE, Bejenaru LE, Varuţ MC, Balasoiu RM, Calina D, Stoian AC, Baluşescu G, Herea DD, Ciocilteu MV, Bita A, Mogoşanu GD and Bejenaru C (2025). Sprayable hybrid gel with cannabidiol, hyaluronic acid and colloidal silver: A multifunctional approach for skin lesion therapy. *Pharmaceutics*, **17**(9).

Dai Z, Yang H, Yin P, Liu X, Zhang L, Dou Y and Sun S (2025). Applications of cyclodextrin-based drug delivery systems in inflammation-related diseases.*Pharmaceutics*, **17**(3): 378.

Dalmora ME, Dalmora SL and Oliveira AG (2001). Inclusion complex of piroxicam with β-cyclodextrin and incorporation in cationic microemulsion. In vitro drug release and *in-vivo* topical anti-inflammatory effect. *Int. J. Pharm.*, **222**(1): 45-55.

de Souza JF, Silvestri S, de Souza PR, Fajardo AR and Iglesias BA (2025). Combined cyclodextrins and porphyrinoid derivatives in drug delivery systems: Developments and perspectives. *Int. J. Pharm.*, **126544**.

Del Valle EM (2004). Cyclodextrins and their uses: A review. *Process Biochem.*, **39**(9): 1033-1046.

Dong E, Huo Q, Zhang J, Han H, Cai T and Liu D (2025). Advancements in nanoscale delivery systems: Optimizing intermolecular interactions for superior drug encapsulation and precision release. *Drug Deliv. Transl. Res.*, **15**(1): 7-25.

Dzhardimalieva GI, Rabinskiy LN, Kydralieva KA and Uflyand IE (2019). Recent advances in metallopolymer-based drug delivery systems. *RSC Adv.*, **9**(63): 37009-37051.

Fernandes R and Gracias DH (2012). Self-folding polymeric containers for encapsulation and delivery of drugs. *Adv. Drug Deliv. Rev.*, **64**(14): 1579-1589.

Forsgren J, Frykstrand S, Grandfield K, Mihranyan A and Strømme M (2013). A template-free, ultra-adsorbing, high surface area carbonate nanostructure. *PLoS One*, **8**(7): e68486.

Gao S, Yang G, Zhang X, Lu Y, Chen Y, Wu X and Song C (2022). β-Cyclodextrin polymer-based host–guest interaction and fluorescence enhancement of pyrene for sensitive isocarbophos detection. *ACS Omega*, **7**(15): 12747-12752.

Gjuroski I, Furrer J and Vermathen M (2021). Probing the interactions of porphyrins with macromolecules using NMR spectroscopy techniques. *Molecules*, **26**(7): 1942.

Gote V, Ansong M and Pal D (2020). Prodrugs and nanomicelles to overcome ocular barriers for drug penetration. *Expert Opin. Drug Metab. Toxicol.*, **16**(10): 885-906.

Gupta M, Wahi A, Sharma P, Nagpal R, Raina N, Kaurav M, Bhattacharya J, Rodrigues Oliveira SM, Dolma KG and Paul AK (2022). Recent advances in cancer vaccines: Challenges, achievements and futuristic prospects. *Vaccines*, **10**(12): 2011.

Han Y, Liu W, Huang J, Qiu S, Zhong H, Liu D and Liu J (2018). Cyclodextrin-based metal-organic frameworks (CD-MOFs) in pharmaceutics and biomedicine. *Pharmaceutics*, **10**(4): 271.

Harriman A, Kubo Y and Sessler JL (1992). Molecular recognition via base pairing: Photoinduced electron transfer in hydrogen-bonded zinc porphyrin–benzoquinone conjugates. *J. Am. Chem. Soc.*, **114**(1): 388-390.

Huang Y, Jin Q, Wang W, Zhang Y, Geng P, Yang X, Luo D and Xiao S (2026). Nanoengineering of porphyrin-based biomaterials for innovative cancer therapy. *Chem. Rec.*, **26**(5): e202500306.

Ikeda A, Satake S, Mae T, Ueda M, Sugikawa K, Shigeto H, Funabashi H and Kuroda A (2017). Photodynamic activities of porphyrin derivative–cyclodextrin complexes by photoirradiation. *ACS Med. Chem. Lett.*, **8**(5): 555-559.

Iqbal DN, Khaliq S, Mehdi MZ, Mughram MHA and Ahmed M (2026). Porphyrin/metalloporphyrin and their conjugates: A promising platform for drug delivery. *Mol. Divers.*, **30**(1): 1507-1525.

Jeong EY, Burri A, Lee SY and Park SE (2010). Synthesis and catalytic behavior of tetrakis (4-carboxyphenyl) porphyrin–periodic mesoporous organosilica. *J. Mater. Chem.*, **20**(48): 10869-10875.

Jia X and Williams R (2024). 3D-measurement of particles and particulate assemblies – A review of the paradigm shift in describing anisotropic particles. *Powder Technol.*, **447**: 120109.

Jug M, BeciRevic-Lacan M, Kwokal A and Cetina-Cizmek B (2005). Influence of cyclodextrin complexation on piroxicam gel formulations. *Acta Pharm.*, **55**(3): 223-236.

Kandambeth S, Shinde DB, Panda MK, Lukose B, Heine T and Banerjee R (2013). Enhancement of chemical stability and crystallinity in porphyrin-containing covalent organic frameworks by intramolecular hydrogen bonds. *Angew. Chem. Int. Ed.*, **52**(49): 13290-13294.

Kargari Aghmiouni D and Khoee S (2023). Dual-drug delivery by anisotropic and uniform hybrid nanostructures: A comparative study of the function and substrate–drug interaction properties. *Pharmaceutics*, **15**(4): 1214.

Karlsson J, Vaughan HJ and Green JJ (2018). Biodegradable polymeric nanoparticles for therapeutic cancer treatments. *Annu. Rev. Chem. Biomol. Eng.*, **9**: 105-127.

Khatoon H, Faudzi SMM and Sohajda T (2025). Mechanisms and therapeutic applications of β-cyclodextrin in drug solubilisation and delivery systems. *Chem. Biodivers.*, **22**(11): e00359.

Kim J, Lee Y, Kim Y, Rha H, Kim D, Debnath S, Pu K, Kang H and Kim JS (2025). Site-specific transformable nanostructures for cancer therapy and diagnosis. *Chem. Rev.*, **125**(18): 9012-9052.

Korsmeyer RW, Gurny R, Doelker E, Buri P and Peppas NA (1983). Mechanisms of solute release from porous hydrophilic polymers. *Int. J. Pharm.*, **15**(1): 25-35.

Lakshani N, Wijerathne H, Sandaruwan C, Kottegoda N and Karunarathne V (2023). Release kinetic models and release mechanisms of controlled-release and slow-release fertilizers. *ACS Agric. Sci. Technol.*, **3**(11): 939-956.

Lehn JM (1995). Supramolecular chemistry: Concepts and perspectives. John Wiley & Sons.

Lestari WW, Suwarno H and Arrozi USF (2019). Spillover effect on Pd-embedded metal-organic frameworks based on zirconium (IV) and benzene-1,3,5-tricarboxylate as hydrogen storage materials. *Mater. Res. Express*, **6**(8): 084001.

Li X, Fu L, Chen F, Lv Y, Zhang R, Zhao S and Karimi-Maleh H (2025). Cyclodextrin-based architectures for electrochemical sensing: From molecular recognition to functional hybrids. *Anal. Methods*, **17**(21): 4300-4320.

Likhonina AE, Mamardashvili GM, Khodov IA and Mamardashvili NZ (2023). Synthesis and design of hybrid metalloporphyrin polymers based on palladium (II) and copper (II) cations and axial complexes of pyridyl-substituted Sn (IV) porphyrins with octopamine. *Polymers*, **15**(4): 1055.

Lionis A, Peppas K, Nistazakis HE, Tsigopoulos A and Cohn K (2021). Statistical modeling of received signal strength for an FSO link over maritime environment. *Opt. Commun.*, **489**: 126858.

Massiot D, Alonso B, Fayon F, Fredoueil F and Bujoli B (2001). New NMR developments for structural investigation of proton-bearing materials at different length scales. *Solid State Sci.*, **3**(1–2): 11-16.

Mavridis IM and Yannakopoulou K (2019). Porphyrinoid–cyclodextrin assemblies in biomedical research: An update. *J. Med. Chem.*, **63**(7): 3391-3424.

Miranda GM, Santos VORe, Bessa JR, Teles YC, Yahouedehou SCMA, Goncalves MS and Ribeiro-Filho J (2021). Inclusion complexes of non-steroidal anti-inflammatory drugs with cyclodextrins: A systematic review. *Biomolecules*, **11**(3): 361.

Mirza S, Miroshnyk I, Habib MJ, Brausch JF and Hussain MD (2010). Enhanced dissolution and oral bioavailability of piroxicam formulations: Modulating effect of phospholipids. *Pharmaceutics*, **2**(4): 339-350.

Monteiro CJ, Neves MG, Nativi C, Almeida A and Faustino MAF (2023). Porphyrin photosensitizers grafted in cellulose supports: A review. *Int. J. Mol. Sci.*, **24**(4): 3475.

Nisa K, Lone IA, Arif W, Singh P, Rehman SU and Kumar R (2023). Applications of supramolecular assemblies in drug delivery and photodynamic therapy. *RSC Med. Chem.*, **14**(12): 2438-2458.

Ouahab L (1997). Organic/inorganic supramolecular assemblies and synergy between physical properties. *Chem. Mater.*, **9**(9): 1909-1926.

Peppas K, Alexandropoulos G, Datsikas C and Lazarakis F (2011). Multivariate gamma–gamma distribution with exponential correlation and its applications in radio frequency and optical wireless communications. *IET Microw. Antennas Propag.*, **5**(3): 364-371.

Peppas KP, Lazarakis F, Alexandridis A and Dangakis K (2012). Simple, accurate formula for the average bit error probability of multiple-input multiple-output free-space optical links over negative exponential turbulence channels. *Opt. Lett.*, **37**(15): 3243-3245.

Quadrado RF, Vitoria HF, Ferreira DC, Krambrock K, Moreira KS, Burgo TA, Iglesias BA and Fajardo AR (2022). Hybrid polymer aerogels containing porphyrins as catalysts for efficient photodegradation of pharmaceuticals in water. *J. Colloid Interface Sci.*, **613**: 461-476.

Raffaini G and Ganazzoli F (2020). Understanding surface interaction and inclusion complexes between piroxicam and native or crosslinked β-cyclodextrins: The role of drug concentration. *Molecules*, **25**(12): 2848.

Redasani VK, Patel PR, Marathe DY, Chaudhari SR, Shirkhedkar AA and Surana SJ (2018). A review on derivative UV-spectrophotometry analysis of drugs in pharmaceutical formulations and biological samples. *J. Chil. Chem. Soc.*, **63**(3): 4126-4134.

Ritger PL and Peppas NA (1987). A simple equation for description of solute release II: Fickian and anomalous release from swellable devices. *J. Control. Release*, **5**(1): 37-42.

Samanthula KS, Obbalareddy S, Thatipelli RC and Bairi AG (2024). Solid lipid nanoparticles for the delivery of plant-derived bioactive compounds in the treatment of cancer disorders—A review. *J. Nat. Remedies*.

Sarkar M, Khandavilli S and Panchagnula R (2006). Development and validation of RP-HPLC and ultraviolet spectrophotometric methods of analysis for the quantitative estimation of antiretroviral drugs in pharmaceutical dosage forms. *J. Chromatogr. B*, **830**(2): 349-354.

Scarpignato C (2013). Piroxicam-β-cyclodextrin: A GI safer piroxicam. *Curr. Med. Chem.*, **20**(19): 2415-2437.

Shan C, Ru J, Zhang M, Cao J, Liu W, Guo H and Tang Y (2019). A novel drug–drug nanohybrid for the self-delivery of porphyrin and cis-platinum. *RSC Adv.*, **9**(63): 37003-37008.

Sharma M, Prasher P, Fatima R, Calina D and Sharifi-Rad J (2025). β-Cyclodextrin-based multifunctional carriers for colon-targeted drug delivery: Advances in hydrogel systems and mucoadhesive strategies. *Cancer Nanotechnol.*, **16**(1): 36.

Shimizu S (2017). Recent advances in subporphyrins and triphyrin analogues: Contracted porphyrins comprising three pyrrole rings. *Chem. Rev.*, **117**(4): 2730-2784.

Silva LB, Castro KA, Botteon CE, Oliveira CL, Da Silva RS and Marcato PD (2021). Hybrid nanoparticles as an efficient porphyrin delivery system for cancer cells to enhance photodynamic therapy. *Front. Bioeng. Biotechnol.*, **9**: 679128.

Tamo AK (2024). Nanocellulose-based hydrogels as versatile materials with interesting functional properties for tissue engineering applications. *J. Mater. Chem. B*, **12**(32): 7692-7759.

Topuz F (2022). Rapid sublingual delivery of piroxicam from electrospun cyclodextrin inclusion complex nanofibers. *ACS Omega*, **7**(39): 35083-35091.

Topuz F and Uyar T (2024). Recent advances in cyclodextrin-based nanoscale drug delivery systems. *Wiley Interdiscip. Rev. Nanomed. Nanobiotechnol.*, **16**(6): e1995.

Uekama K, Hirayama F and Irie T (1998). Cyclodextrin drug carrier systems. *Adv. Drug Deliv. Rev.*.

Xing C, Zheng X, Deng T, Zeng L, Liu X and Chi X (2023). The role of cyclodextrin in the construction of nanoplatforms: From structure, function and application perspectives. *Pharmaceutics*, **15**(5): 1536.

Zhang H, Zhou Y, Pan Z, Wang B, Yang L, Zhang N, Chen B, Wang X, Jian Z, Wang L, Ling H, Qin X, Zhang Z, Liu T, Zheng A, Tan Y, Bi Y and Yang R (2024). Toxicity assessment of Cucurbita pepo cv Dayangua and its effects on gut microbiota in mice. *BMC Complement. Med. Ther.*, **24**: 243.

Zhu W, Lv Y, Yang Q, Zu Y and Zhao X (2022). Artemisinin hydroxypropyl-β-cyclodextrin inclusion complex loaded with porous starch for enhanced bioavailability. *Int. J. Biol. Macromol.*, **211**: 207-217.

Zou Y, Wu J, Zhang Q, Chen J, Luo X, Qu Y, Xia R, Wang W and Zheng X (2024). Recent advances in cell membrane-coated porphyrin-based nanoscale MOFs for enhanced photodynamic therapy. *Front. Pharmacol.*, **15**: 1505212.